Sensors and Actuators A 156 (2009) 88–94

Contents lists available at ScienceDirect

Sensors and Actuators A: Physical

journal homepage: www.elsevier.com/locate/sna

Uncooled infrared thermo-mechanical detector array: Design, fabrication and testing

M. Fatih Toy [a], Onur Ferhanoglu [a,*], Hamdi Torun [b], Hakan Urey [a]

[a] Koc University, Electrical and Electronics Eng. Dept., Istanbul, Turkey
[b] Georgia Institute of Technology, The George W. Woodruff School of Mechanical Engineering, Atlanta, USA

ARTICLE INFO

Article history:
Received 29 September 2008
Received in revised form
23 December 2008
Accepted 16 February 2009
Available online 28 February 2009

Keywords:
Thermal detector
NETD
Optical readout
Diffraction grating
CCD camera

ABSTRACT

Thermo-mechanical detector arrays in the 160 × 120 array format are designed, fabricated, and tested. Detectors are composed of SiN_x and TiN as absorbing layer, Al to form bimaterial legs, and integrated diffraction grating interferometer underneath each detector. The detector array is a passive component and the optical readout is performed remotely with a laser and CCD camera. All noise sources are considered in making a detailed noise equivalent temperature difference (NETD) estimation, which revealed <30 mK NETD is achievable using >12-bit CCD camera for the readout.

1. Introduction

Infrared (IR) detectors find applications in many areas such as medical imaging, rescue and security, military, electrical/mechanical system temperature monitoring. Thermal imagers can be divided into two main categories: photon detectors (cooled) and thermal detectors (uncooled). Cooled thermal detectors work with very high sensitivity, on the expense of cryogenic cooling requirement which requires high power, therefore cooled detectors are used where performance is the main issue, such as heavy weapon platforms and astronomy [1]. On the other hand, uncooled thermal detectors are lower in sensitivity; however; they are attractive since they require no cooling and can be fabricated within only several masks. Operation principle of uncooled thermal detectors is based on the modulation of an electrical, optical or mechanical parameter with absorbed IR radiation. Theoretical analysis shows that the performance of uncooled thermal detectors can potentially be increased up to cooled thermal detector performance level by incorporating optical readout into bimaterial MEMS structures that bend in response to IR radiation [2].

This paper discusses the design, fabrication, and testing of an uncooled infrared thermo-mechanical detector array [2–6] with integrated diffraction grating underneath each detector. The proposed design has the advantage of decoupling the thermo-mechanical sensor array from the readout, providing optimal design of each part to achieve low minimum detectable temperature. In addition, detector array requires no electrical connections to the substrate and can be microfabricated with only 4 masks. The array is immune to saturation while observing high temperature targets by incorporating readout algorithms to extend the range of optical interferometry. Diffraction grating based readout is proven to achieve sub-nm precision for detecting small mechanical deflections [7].

2. Theory

Fig. 1 illustrates the basic principle of the thermo-mechanical IR detector array. Details of the device will be further provided in the detector design section. The design is based on optical detection of mechanical motion of the bimaterial detector array with absorbed IR radiation. Bending of the MEMS detectors is achieved via the bimaterial legs connected to the absorption membrane. This bending is measured from the backside of the transparent substrate with embedded diffraction gratings and reflector on each detector. As the detectors bend, the diffracted 1st order lights from each detector are modulated.

Theoretical analysis of such a system requires a broader perspective. The IR radiation emitted from an object first undergoes atmospheric effects, then is imaged onto the sensor array through an IR lens, as illustrated in Fig. 2.

In IR detectors, the detector temperature is only a small fraction of the target temperature T_t and can be expressed in terms of the

* Corresponding author. Tel.: +90 212 338 1772; fax: +90 212 338 1548.
E-mail address: oferhanoglu@ku.edu.tr (O. Ferhanoglu).

0924-4247/$ – see front matter
doi:10.1016/j.sna.2009.02.010

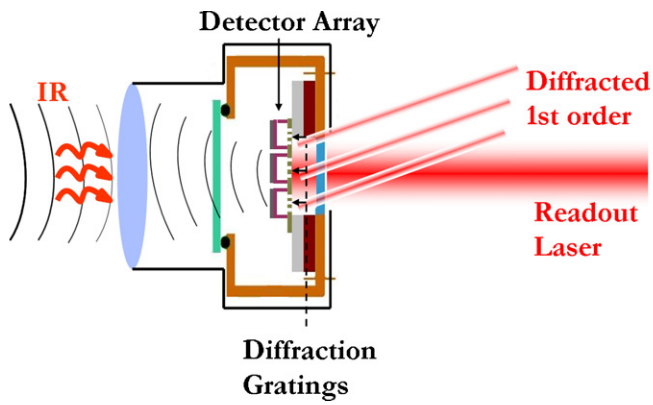

Fig. 1. Basic principle: mechanical bending of the detector array due to absorbed IR radiation is monitored from the back side by observing 1st diffracted orders from diffraction gratings embedded underneath each detector.

parameters illustrated in Fig. 2 [3]:

$$\Delta T = \underbrace{\frac{\eta\tau_0 A_d (\mathrm{d}P/\mathrm{d}T)_{\lambda_1-\lambda_2}}{4F_\#^2 G}}_{K} T_t \tag{1}$$

where the factor $(\mathrm{d}P/\mathrm{d}T)_{8-14}$ $(\mathrm{W\,m^{-2}\,K^{-1}})$ is the radiated power change per temperature change, integrated between the wavelengths of interest, long wave IR (LWIR) defined as the 8–14 μm band. τ_0 is the atmospheric, $F_\#$ is the *f*-number of IR Lens, A_d is the detector area, η is the detector absorbance and G (W/K) is the thermal conductivity of the detector. K is the conversion ratio between T_t and ΔT.

The detector displacement can be calculated by multiplying each side of Eq. (1) with $\Delta z/\Delta T$-ratio (vertical detector displacement per unit temperature difference), which is a design parameter:

$$\Delta z = \frac{\Delta z}{\Delta T} K T_t \tag{2}$$

3. Noise sources

The performance of a thermo-mechanical detector is determined by a number of noise sources that will be described in detail in this section. Noise in any kind, in return will create disturbance in the displacement of the detector: $\langle\delta z\rangle^{1/2}$. Signal-to-noise ratio (SNR) may be written as

$$\frac{\Delta z}{\langle\delta z^2\rangle^{1/2}} = \frac{\Delta z}{\Delta T}\frac{KT_t}{\langle\delta z^2\rangle^{1/2}} \tag{3}$$

Finally, noise equivalent temperature difference (NETD) is the target temperature T_t at which the SNR is unity:

$$\mathrm{NETD} = \frac{\langle\delta z^2\rangle^{1/2}}{K(\Delta z/\Delta T)} \tag{4}$$

The four fundamental noise sources can formulated as [3]:

(1) *Thermal fluctuation noise* (*TF*): caused due to conductive heat exchange between the detector and the substrate

$$\langle\delta z^2\rangle_{TF}^{1/2} = \frac{\Delta z}{\Delta T}\langle\delta T^2\rangle_{TF}^{1/2} = \frac{\Delta z}{\Delta T} T\sqrt{\frac{4k_B B}{G}} \tag{5}$$

where k_B is Boltzmann's constant and B is measurement bandwidth (Hz).

(2) *Thermo-mechanical noise*: caused by the continuous exchange of mechanical energy and thermal energy of environment

$$\langle\delta z^2\rangle_{TM}^{1/2} = \sqrt{\frac{4k_B TB}{Qkw_0}} \tag{6}$$

where T is the ambient temperature of the detector array package (K) and Q, k and w_0 are the quality factor, stiffness (N/m) and resonant frequency (Hz) of the thermo-mechanical detector respectively.

(3) *Background fluctuation noise*: radiative heat exchange between the pixel and the surrounding. It constitutes the fundamental limit of thermal detector performance

$$\langle\delta z^2\rangle_{BF}^{1/2} = \frac{\Delta z}{\Delta T}\frac{2}{G}\sqrt{2k_B\sigma_T B(T_D^5 + T^5)A_d} \tag{7}$$

where T_D is the detector temperature and σ_T is Stephan–Boltzmann constant.

(4) *Readout noise*: contribution of the readout electronics and optics [2]

$$\langle\delta z^2\rangle_{RO}^{1/2} = \frac{n_{CCD}}{S_{CCD}} \tag{8}$$

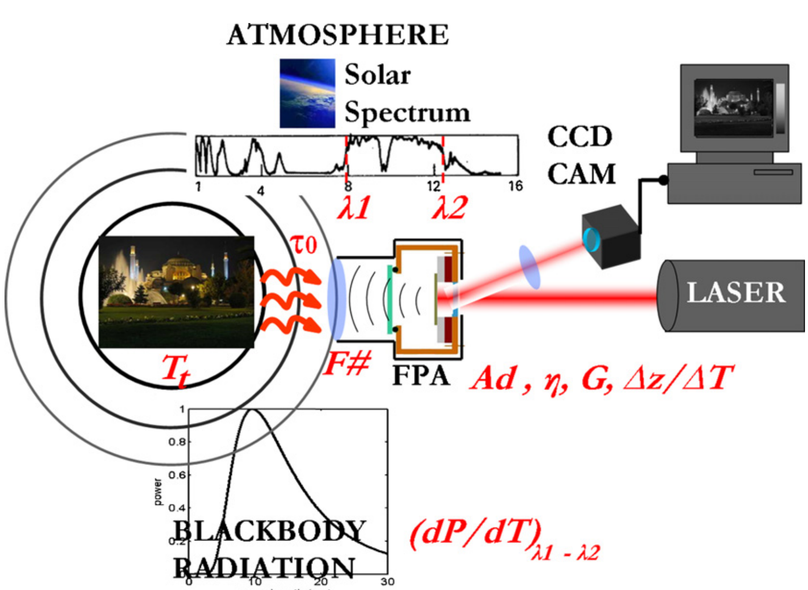

Fig. 2. Big picture showing IR imaging and backside optical readout.

where n_{CCD} is the noise of the CCD camera in CCD units and S_{CCD} is the sensitivity of the detector, i.e. the ratio of readout intensity variation in the CCD units per unit deflection of the detector. In NETD calculations, a 12-bit CCD camera with n_{CCD} 1-bit noise level is assumed. Total NETD is found using:

$$\mathrm{NETD} = \frac{\sqrt{\langle \delta z^2 \rangle_{TF}^2 + \langle \delta z^2 \rangle_{TM}^2 + \langle \delta z^2 \rangle_{BF}^2 + \langle \delta z^2 \rangle_{RO}^2}}{K \frac{\Delta z}{\Delta T}} \tag{9}$$

In NETD calculations; $A_d = \beta 50\,\mu\mathrm{m} \times 50\,\mu\mathrm{m}$ (β: fill factor of the detector), $\tau_0 = 0.9$ for 8–14 μm gap, $\eta = 0.5$ $(\mathrm{d}P/\mathrm{d}T)_{8-14} = 2.62$ $(\mathrm{W\,m^{-2}\,K^{-1}})$, $F_{\#} = 1$, $B = 30$ Hz is assumed. k, w_0, G, and $\Delta z/\Delta T$ are obtained using ANSYS^{TM} finite element modeling software. Q is taken as 500 in vacuum as a reasonable approximation [3].

4. Grating interferometry

Diffraction gratings provided sensitive displacement measurements for MEMS sensors, such as AFM, thermal imagers and acoustic transducers [7–9]. Fig. 3 illustrates the backside optical readout of a single thermo-mechanical IR detector. Bending due to IR absorption is monitored by detecting 1st order diffracted light.

The intensity of 1st order changes sinusoidally with respect to gap:

$$I_1 \alpha \sin^2\left(\frac{2\pi}{\lambda} d\right) \tag{10}$$

where I_1 is the intensity of 1st diffracted order, λ is the readout wavelength and d is the gap between the reflector and grating.

5. Mechanical designs

Structural layer of the detectors are chosen to be silicon nitride (SiN_x), which is also a good IR absorber. Aluminum is used as bimaterial metal, providing good thermal mismatch with SiN_x and as an optical reflector for backside readout. The reflector and the diffraction grating underneath form an interferometer [10].

Mask layout of the mechanical designs is provided in Fig. 4. Designs 1-a and 1-b are crab leg designs with different number of joints. Group 2 (a, b, c) is cantilever type detectors with different bimaterial lengths.

Group 3 (a, b, c) has oppositely placed legs to achieve parallel mechanical displacement; with different bimaterial lengths. The mechanical designs are optimized to have NETD values <100 mK.

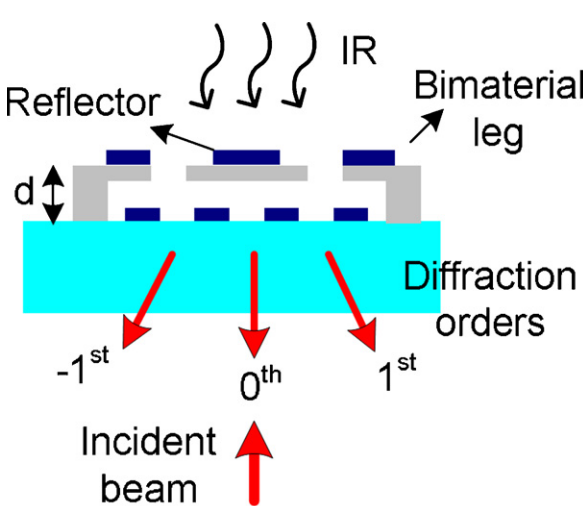

Fig. 3. Optical readout of a single thermo-mechanical IR detector.

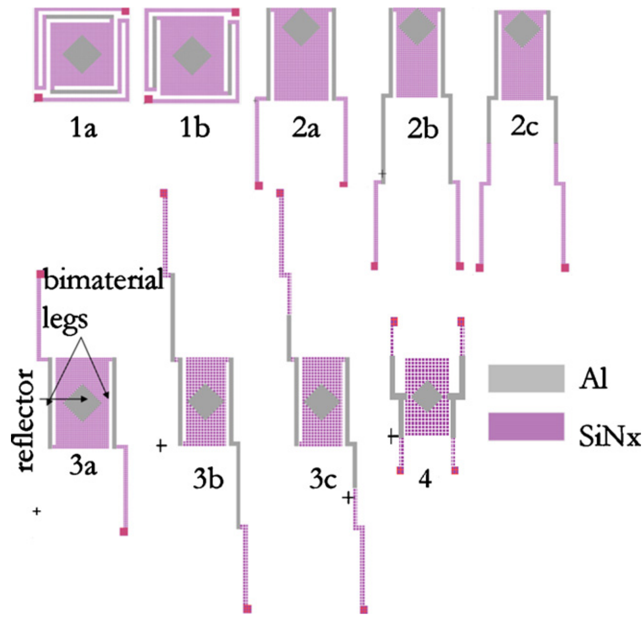

Fig. 4. Layout for the designed detectors.

NETD values for all the designs were calculated with given formulations and are tabulated in Table 1.

Fill factors for all designs lay in between 35% and 45%. Time constant τ_D of the detectors are calculated using:

$$\tau_D = \frac{\rho c V}{G} \tag{11}$$

where ρ is the density, c is the heat capacity and V is the volume. To find the time constant; the density, heat capacity and volume multiplication of each material on the detector is added. The summation is divided by the thermal conductivity of the legs.

Time constants of the designs are around 3 ms, which makes the array suitable for 30 fps, and also for frame rates up to 200 fps in some designs. Deflections vary between 25 nm up to almost 375 nm per K of temperature change at the detector. Adding up all the noise components, assuming a 12-bit CCD camera gives sufficiently low NETD values, <100 mK for most of the designs. NETD values are much lower for a 14-bit CCD camera.

6. Fabrication

Fabrication was carried out at Middle East Technical University, Microelectronics Center (METU-MET) in Turkey. Fabrication steps are illustrated in Fig. 5. First, gold gratings are evaporated and patterned onto pyrex substrate. Polyimide is deposited as sacrificial material. Thickness of the polyimide layer is chosen to be quarter of the IR wavelength; 2–2.5 μm, as a resonant gap for optimum absorption. 200 nm SiN_x and 300 nm aluminum is deposited. A thin layer of titanium nitride (TiN) is deposited after patterning of aluminum layer, to enhance IR absorption. Finally SiN_x is patterned, and the device is released with oxygen plasma etch.

Fig. 6 illustrates microscope and SEM images from fabricated detector arrays. Light gray regions are aluminum (reflector and bimaterial legs). Fringes indicate residual stress causing warping of the detectors after release. However, the area surrounding the center Al reflector seems to be flat.

7. IR absorption

As previously mentioned, absorption layer of the detectors is composed of SiN_x, a common absorber for thermo-mechanical

Table 1
NETD performance of designed detectors (nearest integer in mK).

Design	1a	1b	2a	2b	2c	3a	3b	3c	4c
Fill factor	43%	34%	46%	35%	35%	46%	34%	34%	46%
Time constant (ms)	3.7	5	2	1.7	2.3	2	1.7	2.3	0.7
Deflection (nm/K)	25	25	55	275	150	128	373	310	25
$NETD_{TF}$ (mK)	13	13	17	23	20	18	23	20	32
$NETD_{TM}$ (mK)	29	20	16	39	71	9	8	8	11
$NETD_{BF}$ (mK)	3	3	3	3	3	3	3	3	2
NETD (mK) 12-bit CCD	127	125	107	53	83	49	33	29	83
NETD (mK) 14-bit CCD	45	42	35	46	75	23	26	23	39

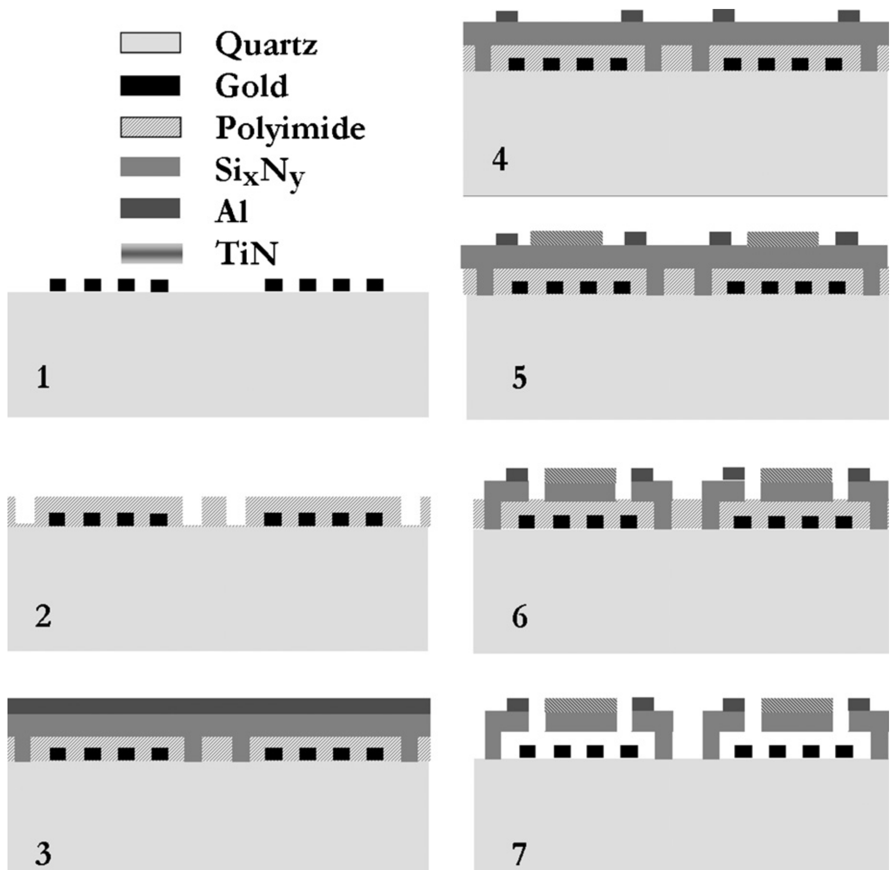

Fig. 5. Fabrication steps: (1) patterning of gold gratings, (2) polyimide spinning and definition of anchors, (3) SiN_x and Al deposition, (4) Al patterning, (5) TiN deposition and patterning, (6) SiN_x patterning, and (7) release.

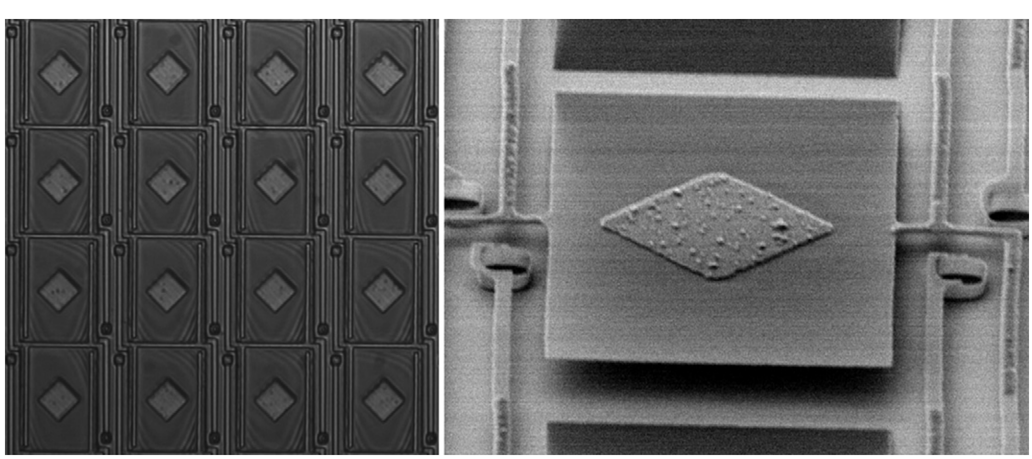

Fig. 6. Microscope and SEM images from the fabricated detector array.

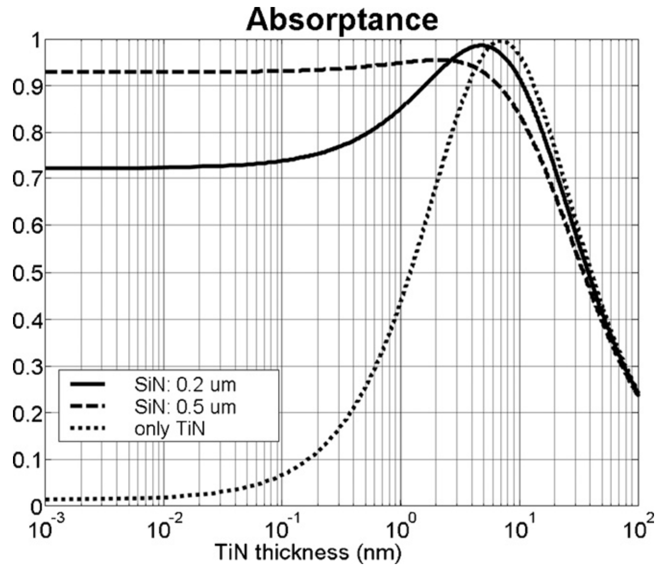

Fig. 7. Absorption characteristics of the detector with TiN and Si_xNy layers.

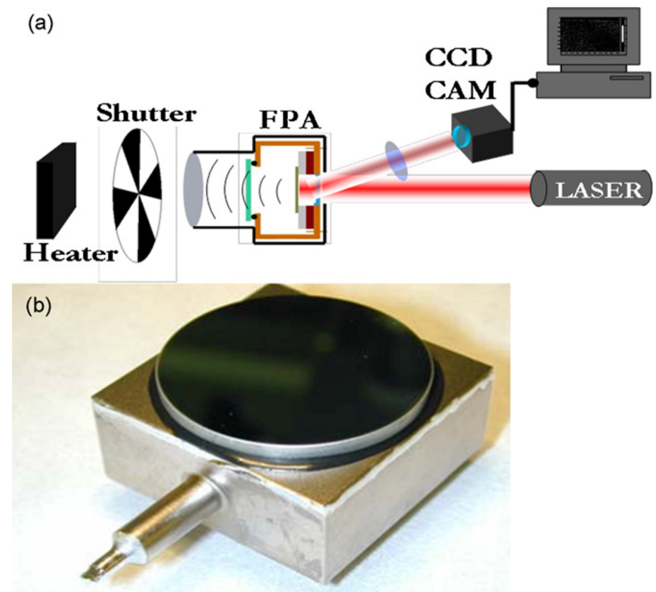

Fig. 8. (a) Experimental setup. (b) Vacuum package for detector array.

IR detectors [2–6]. However high absorption values can only be achieved with SiN_x layers of near 0.5 μm [9]. Our design approach was to use a 0.2 μm SiN_x layer to achieve high mechanical deflection. The absorption was enhanced through a thin layer of TiN.

To investigate absorption of designed detectors, simulations were carried out by calculating Fresnel coefficients for an n-layer medium [9,11]: 5 nm TiN, 0.2 μm SiN_x, 2.5 μm gap, and perfect reflector, respectively. The absorption characteristic is given in Fig. 7.

Maximum absorption is observed for a 5 nm TiN layer ($n = 9.8$ $k = 11.4$) enhancing the absorption of 0.2 μm SiN_x. Simulations were also performed for SiN_x thickness of 0.5 μm and only TiN. It is observed that as the thickness of SiN_x increases, dependence of absorption to TiN thickness decreases, since certain portion of the IR radiation is absorbed by SiN_x. On the other hand, increase of SiN_x thickness would decrease mechanical bending of the structure, lowering the responsivity of the detector, thus increasing NETD. Therefore $SiN_x = 0.2$ μm and TiN = 5 nm were chosen as design points. In fact, it is observed that for 0.2 μm of SiN_x, TiN thickness of 1–10 nm range gives more than 90% absorption. Experimental characterization of the absorption of the array is left as future work.

8. Experimental setup and results

Fabricated detector array, is placed in a vacuum package with two windows; a visible window on the back side for optical readout, and an IR window at the front. Fig. 8 illustrates the experimental setup, and the vacuum package [12] of the detector array. A laser is expanded through a telescope and the diffracted 1st orders are imaged onto an 8-bit CCD camera using a lens. A video is recorded while the target temperature is changed between IR heater temperature ($T + 65$ K) and the reference temperature of the shutter (T). Before the experiment, spatial uniformity and transient behavior of the heater were monitored using an IR thermometer to ensure stability.

Diffracted 1st order light from detectors is imaged onto the CCD camera and illustrated in Fig. 9. Single detector output captured at 1.87 frames-per-second with 33 ms (i.e. 30 Hz detection bandwidth) shutter time is illustrated in Fig. 10. The resultant first order modulation is 987 CCD intensity units and RMS noise is 31.34 CCD

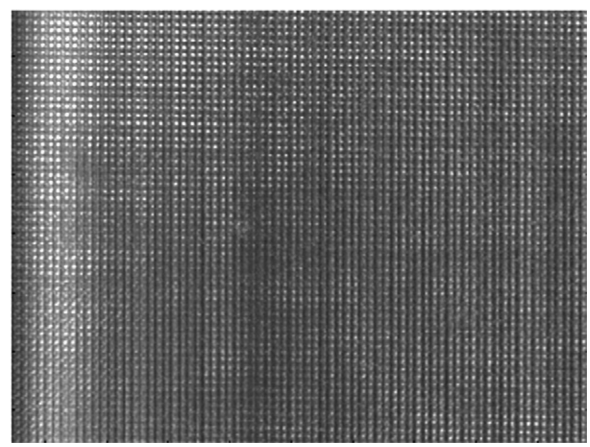

Fig. 9. Imaged 1st order light on CCD camera.

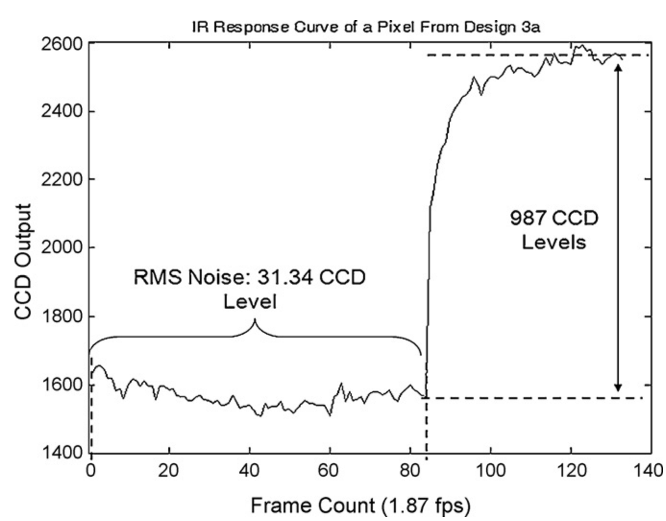

Fig. 10. Response curve of a single detector to the heater. Temperature is increased for 65 K at 85th frame.

intensity units. Experimentally obtained thermal response time is limited with the current setup and is much slower than the response time of the detector structures. The observed response is due to the combination of IR absorption and conductive heat transfer from the heater. Close loop temperature stabilization of the array should be performed in order to report NETD.

The current experimental setup uses an 8-bit CCD camera and provides vacuum sealing of 500–1000 mTorr. Theoretical calculations show that with the current setup, NETD value rises to 1.2 K. However the performance estimation of the detectors given above considers an improved setup that would use a 12-bit CCD and <10 mTorr vacuum sealing for the detectors. We expect to reduce the NETD of the detectors below 100 mK with the improved setup.

The performance of an IR detector array is measured with the "spatial NETD" which considers the variation of the sensitivities within the array. In the past few years thermo-mechanical detector arrays suffered severely from non-uniformities [2,13] and exhibited low spatial NETD. Current studies on thermo-mechanical IR detector arrays reveal that the non-uniformity problems can be better addressed [5,14]. First commercial thermo-mechanical detector array developed by Agiltron Inc. was launched recently and demonstrates that non-uniformity can be controlled [15].

It is possible to further reduce the effect of non-uniformities using two light sources with different wavelengths [16]. Introducing a second light source assures more than 70% of the maximum optical sensitivity with detection range of near 0.5 μm for all array elements. On the other hand, using a single source would give no constraints on the sensitivity and unambiguous detection is limited to less than quarter-wavelength of the light source. Non-uniformities may also be corrected by using a dual grating method, incorporating two-step gratings under the sensor, to avoid low sensitivity regions of the optical curve [17].

9. Conclusions

An uncooled thermal detector with integrated diffraction grating is designed, fabricated and tested. Main advantages of the proposed design are; sensitive interferometric readout and low NETD. The designs are scalable to higher detector resolutions and do not require electrical connections to the substrate. Dynamic range of the detectors can be increased by incorporating readout algorithms to extend the range of optical interferometry, thus preventing saturation.

Future work involves improvement of NETD to near theoretical performance (<50 mK) using a 12-bit CCD camera for the readout, temperature stabilization of the array and demonstration of IR Image acquisition using the full array.

Acknowledgments

This work is sponsored by Aselsan Inc. (Turkey). We are grateful to Prof. Tayfun Akın and Orhan Akar from Middle East Technical University Microelectronics Center: METU-MET for fabrication of the arrays and VTT/Finland for providing vacuum packages. O.F. and M.F.T. acknowledges the support from TUBİTAK scholarship for graduate studies and H.U. acknowledges the support from TÜBA-GEBİP Distinguished Young Scientist award.

References

[1] T. Akin, CMOS-based thermal sensors, in: H. Baltes, O. Brand, G.K. Fedder, C. Hierold, J. Kornivk, O. Tabata (Eds.), Advanced Micro & Nanosystems, vol. 2: CMOS-MEMS, Wiley-VCH, AMN-Flyer, 2005.
[2] Y. Zhao, M. Mao, R. Horowitz, A. Majumdar, J. Varesi, P. Norton, J. Kitching, Optomechanical uncooled infrared imaging system: design, microfabrication, and performance, J. Microelectromech. Syst. 11 (April (2)) (2002) 136–146.
[3] P.G. Datskos, N.V. Lavrik, S. Rajic, Performance of uncooled microcantilever thermal detectors, Rev. Scient. Instrum. 75 (4) (2004).
[4] Y. Zhao, Optomechanical uncooled infrared imaging system, Dissertation for the Degree of Doctor of Philosophy, University of California, Berkeley, Fall 2002.
[5] D. Grbovic, et al., Uncooled infrared imaging using bimaterial microcantilever arrays, Appl. Phys. Lett. 89 (2006) 073118.
[6] L.R. Senesac, et al., imaging using uncooled microcantilever detectors, Ultramicroscopy 97 (2003) 451–458.
[7] H. Torun, J. Sutanto, K.K. Sarangapani, P. Joseph, F.L. Degertekin, C. Zhu, Micromachined membrane-based active probe for biomolecular mechanics measurement, Nanotechnology 18 (2007) 165303.
[8] A.G. Onaran, et al., A new atomic force microscope probe with force sensing integrated readout and active tip, Rev. Scient. Instrum. 77 (2006).
[9] H. Torun, H. Urey, Uncooled thermal camera with optical readout, Opto-Electron. Rev. 14 (2006) 55.
[10] N.A. Hall, F.L. Degertekin, Integrated optical interferometric detection method for micromachined capacitive acoustic transducers, Appl. Phys. Lett. 80 (2002) 3859.
[11] O.S. Heavens, Optical Properties of Thin Solid Films, Butterworths Scientific Publications, London, 1955.
[12] J. Ollila, M.F. Toy, O. Ferhanoglu, P. Karioja, H. Urey, Vacuum package design for a MEMS based IR detector array, in: Proceedings of the European Microelectronics and Packaging Conference, Oulu, 2007.
[13] S.R. Hunter, et al., High sensitivity uncooled microcantilever infrared imaging arrays, in: B.F. Anderson, G.F. Fulop (Eds.), Infrared Technology and Applications XXIX, Proceedings of SPIE, vol. 5074, 2003.
[14] F. Dong, et al., Ultramicroscopy (2007), doi:10.1016/j.ultramic.2007.08.014.
[15] www.agiltron.com.
[16] O. Ferhanoglu, M.F. Toy, H. Urey, Two-wavelength grating interferometry for MEMS sensors, IEEE Photon. Tech. Lett. 19 (2007) 1895–1897.
[17] B. Van Gorp, A.G. Onaran, F.L. Degertekin, Integrated dual grating method for extended range interferometric displacement detection in probe microscopy, Appl. Phys. Lett. 91 (2007) 083101.

Biographies

M. Fatih Toy received BS and MS degrees in electrical and electronics engineering from Koc University, Turkey in 2006 and 2008, respectively. He is currently pursuing a Ph.D. degree in photonics at EPFL. His research interests are MOEMS and 3D imaging.

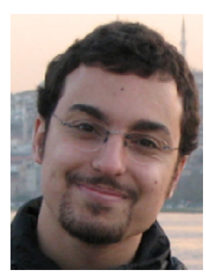

Onur Ferhanoglu received the BS and MSc degrees from Bilkent University, Ankara, Turkey in 2003 and 2005 respectively all in electrical engineering. He joined Optical Microsystems Laboratory in 2005 as a PhD student and research assistant. He has worked as a visiting researcher in the Micromachined Sensors and Transducers Laboratory of Georgia Institute of Technology from September 2007 to March 2008.

His research interests include Optical MEMS, especially thermal imaging and biosensor applications. He is a member of IEEE and SPIE.

Hamdi Torun received the B.S. degree in electrical and electronics engineering from Middle East Technical University, Ankara, Turkey in 2003 and MS degree in electrical and computer engineering from Koc University, Istanbul, Turkey in 2005. He is currently working toward PhD degree in electrical and computer engineering at the Georgia Institute of Technology, Atlanta. His research interests are in design and fabrication of interferometry-based atomic force microscopy probes and thermo-mechanical infrared imagers.

From 2002 to 2003 he was an intern and then a research and development engineer at Aselsan Inc., Ankara, Turkey.

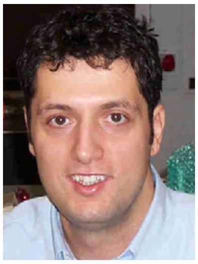

Hakan Urey is an associate professor at Koç University in Istanbul-Turkey. He received the BS degree from Middle East Technical University, Ankara, in 1992, and MS and PhD degrees from Georgia Institute of Technology in 1996 and in 1997, all in electrical engineering. After completing his PhD, he joined Microvision Inc., Seattle as Research Engineer and he played a key role in the development of the Retinal Scanning Display technology. He was the Principal System Engineer when he left Microvision to join the faculty of engineering at Koç University, where he established the Optical Microsystems Research Laboratory (OML).

Dr. Urey has published 7 edited books, 2 book chapters, >20 journal papers, >60 international conference papers, and the inventor of 21 issued >10 pending patents. His research interests are in the area of micro-optics and MEMS for 2D and 3D displays, imaging, and optical, thermal, and biosensors. He is a member of OSA, SPIE, and IEEE-LEOS. He received the Werner Von Siemens faculty excellence award from Koç University in 2006 and the TÜBA (Turkish National Academy of Sciences) Distinguished Young Scientist award in 2007.